Bone Reports 28 (2026) 101889

Contents lists available at ScienceDirect

Bone Reports

journal homepage: www.elsevier.com/locate/bonr

Erythropoietin and bone health: Single high-dose administration triggers bone loss in mice

Anton Gorodov [a], Albert Kolomansky [a,c], Lior Lezerovich [a], Michelle Piper [a], Nathalie Ben-Califa [a], Yankel Gabet [b,*,1], Drorit Neumann [a,*,1]

[a] Department of Cell and Developmental Biology, Gray Faculty of Medical and Health Sciences, Tel Aviv University, Tel Aviv, Israel
[b] Department of Anatomy and Anthropology, Gray Faculty of Medical and Health Sciences, Tel Aviv University, Tel Aviv, Israel
[c] Department of Hematology, Assuta Ashdod University Hospital, Ashdod, Ben-Gurion University, Beer-Sheva, Israel

ARTICLE INFO

Keywords:
Erythropoietin
Osteoclastogenesis
Bone loss
Bone marrow microenvironment
Bone turnover markers
Macrophage colony-stimulating factor

ABSTRACT

Erythropoietin (EPO) is a key regulator of erythropoiesis, and it is mainly used to treat anemia. However, it is also administered prophylactically to non-anemic patients in certain clinical settings and is known to be used illicitly by athletes. The effect of EPO is controversial but emerging evidence indicates that EPO treatment induces bone loss in healthy mice. Here, we investigated the immediate and short-term skeletal effects of a single high-dose EPO injection in young mature (9 weeks) female mice. Cellular and molecular markers of bone turnover were evaluated at multiple time points post-injection. EPO administration led to a rapid increase in macrophage colony-stimulating factor (M-CSF) levels within the bone marrow (BM) microenvironment and in the serum, accompanied by an increase in BM CD115-positive cells and osteoclast precursors, as assessed by flow cytometry. This early cellular response to EPO was followed by an increase in tartrate-resistant acid phosphatase 5b (TRAP5b) and a decrease in procollagen type 1 N-terminal propeptide (P1NP), as determined by serum ELISA analyses, suggesting increased osteoclast numbers and decreased bone formation, respectively. Micro-computed tomography (μCT) revealed a significant reduction in trabecular bone volume. These findings demonstrate that even a single high-dose EPO injection disrupts bone homeostasis and induces significant bone loss through early modulation of the BM niche and osteoclastogenic pathways. Our results have important clinical implications for the prophylactic use of EPO and highlight potential skeletal risks.

1. Introduction

The dynamic nature of bone tissue is characterized by a constant remodeling process (Hadjidakis and Androulakis, 2006). This involves the absorption of bone by osteoclasts, multinucleated cells with a hematopoietic origin, and the concurrent formation of new bone by osteoblasts. These are mononuclear cells originating from mesenchymal stem cells that can evolve into osteocytes, the cells residing within the mineralized matrix. The bone marrow (BM) is a complex network that includes a variety of cell types, such as stromal, endothelial, epithelial, and hematopoietic progenitors. Interactions among these cells play a vital role in bone remodeling by influencing the growth, survival and activity of osteoclasts and osteoblasts, thereby affecting the balance between bone resorption and formation (Šromová et al., 2023).

Erythropoietin (EPO) is a vital glycoprotein hormone that plays a pivotal role in red blood cell production. The hormone is produced primarily in the kidneys in adults and functions by binding the cognate receptor (EPO-R) on erythroid progenitor cells in the BM (Wu et al., 1995). However, in addition to their essential role in erythropoiesis, EPO and EPO-R also affect non-hematopoietic cells, such as endothelial and immune cells (Gassmann et al., 2003; Westenbrink et al., 2007; Kolomansky et al., 2020; Awida et al., 2021; Hiram-Bab et al., 2015; Lipšic et al., 2006; van der Meer and Lipsic, 2006). Activation of EPO-R by EPO elicits several signaling pathways, including Janus kinase 2 (JAK2), signal transducer and activator of transcription 3 or 5 (STAT3/STAT5), mitogen-activated protein kinase (MAPK), protein kinase C (PKC), and phosphatidylinositol 3 kinase/Akt (PI3K/Akt) (Peng et al., 2020). Recombinant forms of EPO are mainly used clinically to treat anemia due to chronic kidney disease and certain hematological malignancies (Panjeta et al., 2015; Forbes et al., 2014; Eckardt et al., 1993).

* Corresponding authors.
E-mail addresses: yankel@tau.ac.il (Y. Gabet), histo6@tauex.tau.ac.il (D. Neumann).
[1] These authors contributed equally to this work.

https://doi.org/10.1016/j.bonr.2025.101889
Received 22 July 2025; Received in revised form 27 October 2025; Accepted 14 November 2025
Available online 18 November 2025

In surgery, particularly major elective procedures, preoperative administration of EPO has been utilized to optimize hemoglobin levels (Ali et al., 2022; Munting and Klein, 2019). This approach aims to reduce the need for allogeneic blood transfusions. Studies have demonstrated that preoperative EPO therapy can effectively increase red blood cell mass, thereby diminishing transfusion requirements and potentially improving surgical outcomes (Cho et al., 2019; Biboulet et al., 2020).

Moreover, athletes, particularly those in endurance disciplines, have misused EPO to enhance performance by increasing the oxygen-carrying capacity of the blood. This practice, known as blood doping, can lead to serious health risks, including increased blood viscosity, which may result in thrombosis or stroke. Consequently, EPO has been banned by the International Olympic Committee (IOC) since 1990, and detection methods have been developed to identify its misuse in athletes (Robinson et al., 2006).

In murine studies, EPO has been associated with divergent skeletal outcomes, spanning from osteogenic stimulation and regeneration, to anti-osteogenic effects such as decreased bone formation and enhanced resorption (Kolomansky et al., 2020; Hiram-Bab et al., 2015; Rauner et al., 2021; Singbrant et al., 2011a; Jung et al., 2008; Li et al., 2015; Cai et al., 2023; Liu et al., 2024). This apparent controversy may derive from a context-dependent outcome of EPO, namely, opposite skeletal actions during bone regeneration and steady-state bone remodeling (see further discussion in (Kolomansky et al., 2020; Hiram-Bab et al., 2015)). Most reports by us and others, agree that in skeletally mature mice at steady-state, high dose EPO treatment induces bone loss (Hiram-Bab et al., 2015; Singbrant et al., 2011a; Suresh et al., 2020a; Rauner et al., 2016). Recent clinical data indicated a significant association between elevated EPO levels and increased bone fracture risk (Kristjansdottir et al., 2020; Suresh et al., 2020b). However, this adverse skeletal effect of EPO is often underestimated and understanding the implications of a biological response to a single, substantial elevation in EPO levels is of prime importance.

Macrophage colony-stimulating factor (M-CSF) is a key cytokine in the development and maintenance of monocytes, macrophages, and associated cells that include osteoclasts (Hume and MacDonald, 2012). M-CSF is produced by cells of mesenchymal and epithelial origins, and the expression is upregulated during inflammation (Hume and MacDonald, 2012). Activation of the M-CSF receptor (M-CSF-R), also known as CD115, sets off signaling cascades that are crucial for cell survival and proliferation (Fleetwood et al., 2016). Signaling pathways activated by M-CSF through M-CSF-R involve nuclear factor-kB (NF-kB), extracellular signal regulated kinases (ERK), and phosphoinositol 3-kinase (PI3K) (Fleetwood et al., 2016).

Although the essential functions of M-CSF and its receptor CD115 in osteoclast development are well established, their specific role in the context of EPO-induced bone remodeling remains underexplored. Recent studies suggest that EPO alters the bone marrow microenvironment in a way that influences osteoclast precursor survival and expansion, thereby modulating M-CSF/CD115 signaling (Hiram-Bab et al., 2015; Rauner et al., 2021; Liu et al., 2024). Understanding this link is critical for clarifying the mechanisms underlying EPO-induced bone loss and provides the rationale for our investigation in the present study.

2. Methods

2.1. Animals

Wild-type 7–9-week old female mice of the inbred strain C57BL/6J-RccHsd were purchased from Envigo (Jerusalem, Israel) and housed in the Tel-Aviv University specific pathogen-free animal facility. Only female mice were used in this study to maintain consistency with our previous investigations of EPO-induced bone remodeling (Kolomansky et al., 2020; Hiram-Bab et al., 2015). This approach ensured comparability across datasets and minimized variability related to sex-specific effects, which were beyond the scope of the present study. We administered 180 units of human recombinant EPO (Epoetin alfa, Eprex®) diluted in 100 μL normal saline for *in vivo* experiments by i.p. injection. Normal saline was used as a diluent control. In all animal experiments, analyses were performed at 9 weeks of age, *i.e.*, the 2-week group was injected at the age of 7 weeks, and the 16-h group was injected ~one day before animals reached 9 weeks of age. Animal care and all relevant procedures were in accordance with the approval of the institutional Animal Care and Use Committee of Tel Aviv University (Permit number TAU-MD-IL-2204-142-3).

2.2. Materials

Antibodies for Western blot detection of M-CSF and GAPDH were purchased from Abcam (Cambridge, UK). ELISA kits for P1NP and TRAP5b were purchased from Immunodiagnostic Systems (UK). An ELISA kit for M-CSF was purchased from ABclonal (USA). Antibodies for flow cytometry were purchased from BioLegend (USA), except for CD115 PE, which was purchased from Miltenyi (Germany); see Table 1.

2.3. Micro-computed tomography (μCT)

The scan settings and morphometric analyses were conducted in accordance with the official guidelines (Bouxsein et al., 2010). Briefly, right femurs (one per mouse) were examined using the Scanco μCT50 system (Scanco Medical AG, Switzerland). The X-ray tube signal is calibrated regularly, and corrections are made as soon as fluctuations exceed 5 %. Scans were performed at a 10 μm nominal resolution, 90 kV energy, 88 μA intensity, and 1000 m/s integration time using a 0.5 mm aluminum filter. The long axis of the femur was placed perpendicular to the X-ray beam axis. The mineralized tissues were segmented using a two-level global thresholding procedure following Gaussian filtration of the stacked tomographic images. The lower threshold for cortical and trabecular bone was defined as 890 mg and 400 mg hydroxyapatite per cm^3, respectively. Morphometric parameters were determined using a direct 3D approach in the secondary spongiosa in the distal metaphysis extending proximally 3 mm from the proximal tip of the primary spongiosa. This region, defined as full metaphysis, was further divided into proximal and distal halves along the main axis of the bone. Changes in the trabecular microarchitecture were assessed by measuring the bone volume fraction (BV/TV), trabecular thickness (Tb.Th), trabecular number (Tb.N), bone mineral density (BMD), trabecular spacing (Tb.Sp.), and connectivity density (Conn.D).

2.4. Hemoglobin

Hemoglobin (Hgb) levels were measured in venous blood (drawn from the facial vein) using a “Mission Plus” hemoglobin/hematocrit meter (Acon, CA, USA).

2.5. Bone marrow extracellular fluid preparation and Western blot analysis

BM samples were collected from femur, tibia, and ilium bones and processed using a previously described centrifugation protocol (Amend

Table 1
Antibodies used for flow cytometry analysis.

Antibody	Source	Identifier
CD11b-APC	BioLegend	Cat#:101211
CD115-PE	Miltenyi Biotec	Cat#:130112828
LY6G-FITC	BioLegend	Cat#: 127605
TER119-FITC	BioLegend	Cat#: 116205
CD3ε-FITC	BioLegend	Cat#: 100305
B220-FITC	BioLegend	Cat#:103205
LY6C- PerCP/Cy5.5	BioLegend	Cat#: 128011

et al., 2016). Briefly, the epiphyses were removed, and the bones were placed into 0.5 mL microcentrifuge tubes in which a hole had been punched using a 21G needle. These tubes were then inserted into 1.5 mL collection tubes prefilled with 100 μL phosphate-buffered saline (PBS) supplemented with a 4 % protease inhibitor cocktail. The samples were centrifuged at 17,000 ×*g* for 1 min. Following centrifugation, the supernatant - referred to as BM extracellular fluid (BM ECF) - and the cellular pellet (BM cells) were collected separately.

For protein analysis, 20 μL of BM ECF was separated by SDS-PAGE using 7.5 % polyacrylamide gels and transferred onto nitrocellulose membranes. The membranes were cut according to the molecular weights of macrophage colony-stimulating factor (M-CSF, 44 kDa) and glyceraldehyde 3-phosphate dehydrogenase (GAPDH, 36 kDa). Membranes were incubated with rabbit anti-mouse M-CSF (1:1000, Abcam, UK) or rabbit anti-mouse GAPDH (1:4000, Abcam, UK) antibodies. Detection was performed using a peroxidase-conjugated goat anti-rabbit secondary antibody (1:10000, Dako, Denmark), with all antibody dilutions prepared in 5 % skim milk. Signal visualization was carried out using the Fusion FX7 imaging system (Vilber Lourmat, France).

2.6. Flow cytometry analysis of bone marrow cells

Bone marrow (BM) cells isolated from the femur, tibia, and ilium of each mouse were pooled into a single sample. Red blood cells were lysed using ACK lysis buffer (Quality Biological, Gaithersburg, MD, USA). Following lysis, BM cells were incubated for 30 min at 4 °C with fluorochrome-conjugated anti-mouse antibodies, as detailed in Table 1. After staining, cells were washed with FACS buffer containing 1 % fetal bovine serum (FBS) and 0.8 % 0.5 M EDTA in PBS. Osteoclast progenitors were defined as Lin^- ($CD3^-$, $B220^-$, $Ly6G^-$, and $TER119^-$) $CD11b^-$ $Ly6C^{high}$ $CD115^+$ cells (Jacome-Galarza et al., 2013; Jacquin et al., 2006; Das et al., 2020). The gates were established by thresholding against unstained controls and confirmed using CD11b single-stained samples to determine the boundary between negative and positive populations. Samples were analyzed using a CytoFLEX flow cytometer, and data were processed with CytExpert 2.4 software (Beckman Coulter, IN, USA).

2.7. Enzyme-linked immunosorbent assay (ELISA)

Levels of TRAP5b and P1NP proteins in mouse serum were quantified using ELISA. Venous blood was collected immediately after euthanasia *via* the vena cava into Microtainer SST tubes (BD, USA), followed by incubation at room temperature for 30 min. Samples were then centrifuged at 17,000 ×*g* for 1.5 min, and the resulting serum was transferred to 1.5 mL tubes. ELISA assays were performed according to the manufacturer's protocols provided with the respective kits.

2.8. Statistical analysis

Results are presented as mean ± standard deviation (SD). To increase statistical power, control groups collected at different time points were pooled, as saline injections were not expected to affect the measured parameters. Before pooling the controls, we performed statistical analysis (normality, one-way ANOVA and Brown–Forsythe) to confirm that controls did not differ significantly across time points. In cases where the control pool did not pass the normality test, we used the nonparametric Mann-Whitney test, otherwise unpaired Student's *t*-test was applied. Kruskal-Wallis and Dunn's test for multiple group comparisons were used to compare more than two groups. Statistical analysis was performed GraphPad Prism 10.1.0 software. $p < 0.05$ determined statistical significance.

3. Results

There is extensive documentation on the erythropoietic effect of EPO, including clinical and experimental studies indicating significant Hgb increase even after a single injection (Lundby et al., 2007; Weltert et al., 2010; Yoo et al., 2012; Rosencher et al., 2005; Singhal et al., 2018). Here, we examined the Hgb levels of mice over two weeks following a single EPO injection of 180 units. Our results indicate that this single administration of EPO induces a significant 13 % increase in Hgb levels within one week (Fig. 1). Hgb levels returned to baseline within two weeks post-injection (Fig. 1).

Since the survival and proliferation of osteoclasts and their precursors depend on M-CSF, we investigated whether EPO administration alters M-CSF protein levels in the BM microenvironment. To this end, we quantified M-CSF levels in BM extracellular fluid (BM ECF) at various time points following a single EPO injection. Western blot analysis revealed a significant 1.7- to 2-fold increase in M-CSF levels as early as 16 h post-injection, which returned to baseline by 48 h (Fig. 2A and B). This transient surge in M-CSF was confirmed by ELISA (Fig. 2C). Notably, by two weeks post-injection, M-CSF levels in BM ECF had decreased by approximately 65 % relative to baseline, suggesting the involvement of a negative feedback mechanism (Fig. 2A). Moreover, the EPO-induced elevation in M-CSF was not restricted to the BM compartment; serum levels of M-CSF were also significantly increased—by 2.8-fold—16 h after EPO injection ($p < 0.05$; Fig. 2D).

Next, we examined the effect of the EPO-induced M-CSF surge on the expression of the M-CSF receptor (CD115) on BM myeloid cells using flow cytometry. Our analysis revealed a significant increase of 32.2 % and 39.8 % in the proportion of $CD115^+$ cells at 48 h and 1 week after EPO administration, respectively (Fig. 3A). Interestingly, among the CD115-positive population, the mean fluorescence intensity (MFI) of CD115 decreased by 24.8 % and 22.4 % at 16 and 48 h post-injection, respectively, suggesting that while a larger number of cells expressed CD115, the receptor's expression level per cell was reduced on average (Fig. 3B).

The increase in $CD115^+$ cells in the BM following a single EPO injection is particularly noteworthy, as we previously reported an elevation in osteoclast progenitor levels after a standard high-dose EPO regimen administered every other day for one week (Awida et al., 2021). Osteoclast progenitors are defined as Lin^- ($CD3^-$, $B220^-$, $Ly6G^-$, and

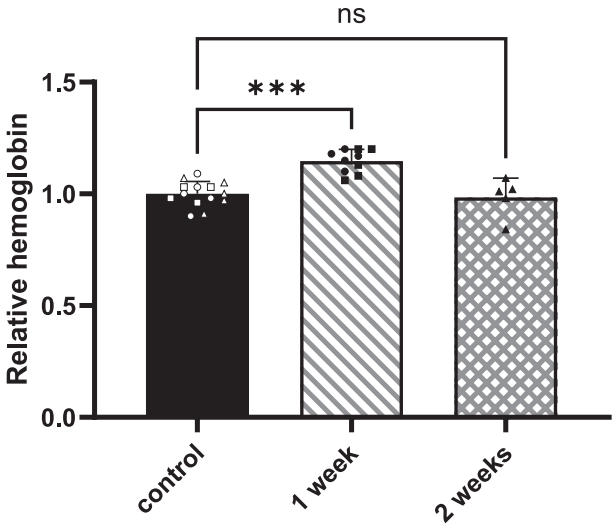

Fig. 1. Erythroid response in EPO-treated mice at 1 and 2 weeks following a single EPO injection.
Hemoglobin levels were measured at 1 and 2 weeks after a single EPO injection and normalized to the corresponding controls. The 1-week data includes both an independent 1-week cohort (square) and the cohort that was followed longitudinally to 2 weeks (circle). The 2-week data reflects measurements from this longitudinal cohort at 2 weeks (triangle). Results are presented as mean ± SD. Statistical significance: ns – not significant; *$p < 0.05$.

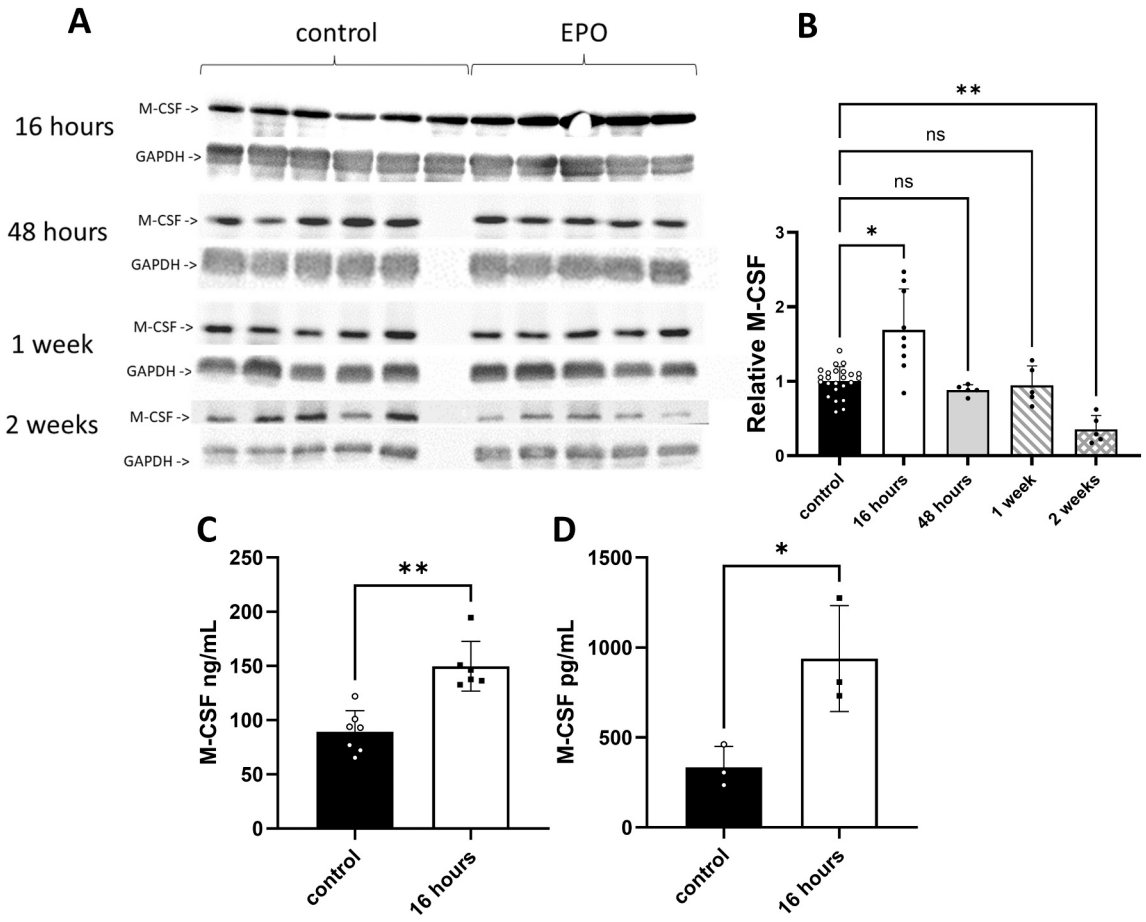

Fig. 2. M-CSF levels in the BM extracellular fluid and serum of EPO-treated mice *vs.* control following a single 180 units EPO injection. A. Representative Western Blot of BM ECF samples; each lane corresponds to an individual mouse. GAPDH was used as an internal protein loading control. B. Quantification of M-CSF levels based on the blot shown in A, including a repeat for the 16-h time point. M-CSF levels were normalized to respective GAPDH levels. C M-CSF levels in BM ECF 16 h after EPO treatment, measured by ELISA and presented in ng/mL. D. M-CSF levels in serum 16 h post-EPO injection, measured by ELISA and presented in pg/mL. Data are presented as mean ± SD. Statistical significance: ns – not significant; $^{**}p < 0.01$; $^{***}p < 0.001$.

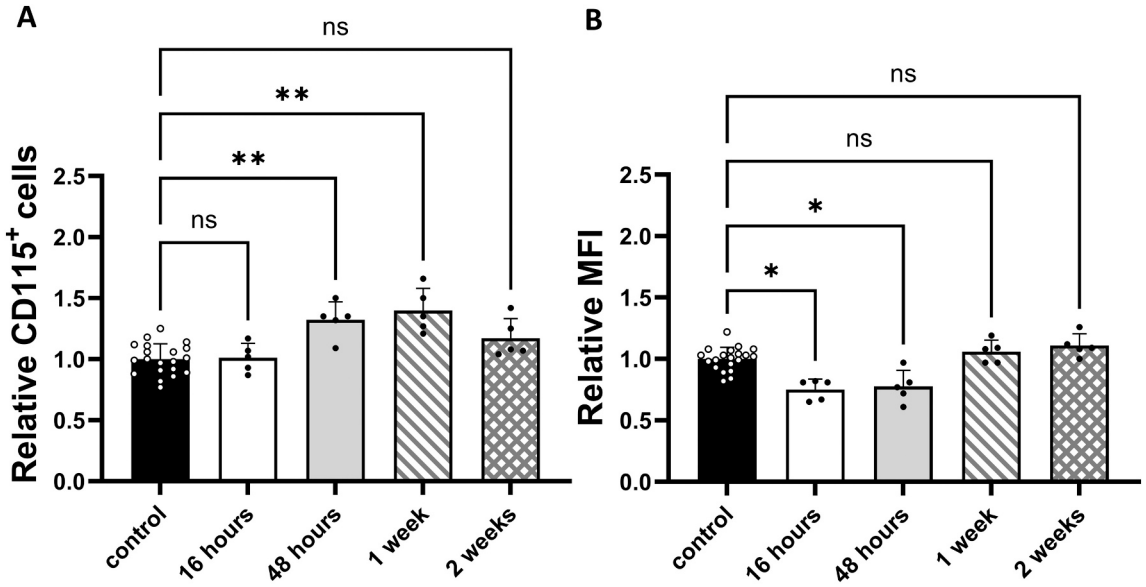

Fig. 3. Flow cytometry analysis of $CD115^+$ cells in the BM of EPO-treated mice *vs* control at the designated time points after a single EPO injection. Data are presented as cell percentage from total BM readout, relative to control. A. Percentage of $CD115^+$ out of total BM cells. B. Corresponding relative CD115 mean fluorescence intensity (MFI) within the gated $CD115^+$ cell population. Data are mean ± SD. ns – nonsignificant, $^{*}p < 0.05$, $^{**}p < 0.01$.

TER119^{-}) CD11b^{-} Ly6C^{high} CD115^{+} cells (Das et al., 2020). Our time-course flow cytometry analysis revealed a significant increase in osteoclast progenitors by 46.5 % at 2 days, 45 % at 1 week, and 87.2 % at 2 weeks post-EPO injection relative to baseline levels (Fig. 4A). Interestingly, the CD115 MFI of the preosteoclasts population increased by 28 % 1 week after EPO injection and returned to baseline levels by 2 weeks (Fig. 4B).

To assess whether the observed increase in osteoclast progenitors is accompanied by a rise in mature osteoclast numbers, we measured serum levels of tartrate-resistant acid phosphatase 5b (TRAP5b), a well-established surrogate marker for mature osteoclast abundance (Alatalo et al., 2000). To account for potential effects of bleeding and diurnal variation on serum markers, EPO-injected mice were compared to saline-injected controls at each corresponding time point (Tsang et al., 2019). At 1-week time point there was a 19.4 % increase in TRAP5b levels, which merged with control levels by the end of the second week. Since EPO is also known to affect osteoblasts (Li et al., 2015; Suresh et al., 2020a; Guo et al., 2014), we measured serum levels of procollagen type 1 N-terminal propeptide (P1NP), a marker of bone formation (Melkko et al., 1996). We observed a marked (82.9 %) reduction in serum P1NP levels at 2 days post-EPO injection (Fig. 5B) followed by a return to control levels at 1 and 2 weeks post-injection. These findings suggest that the effect of EPO on osteoblasts is transient and resolves between days 3 and 7 following injection.

Three-dimensional (3D) micro-computed tomography (μCT) analysis of bone 1 week after EPO injection revealed a 32.8 % loss of trabecular bone volume fraction (BV/TV) and a 22.3 % reduction in trabecular number (Tb. N.), with no significant changes in trabecular thickness (Tb. Th.). These BV/TV and Tb. N. values remained significantly low even after 2 weeks. Notably, there was a partial recovery of Tb.Th (15.3 % increase) 2 weeks after EPO injection, mostly in the distal half of the metaphysis, close to the growth plate (Fig. 6A). These findings were confirmed by additional bone parameters presented in Table 2 and clearly identify a trabecular thickening in the distal half of the metaphysis, also seen in the 3D reconstruction images of the proximal femur (Fig. 6B).

4. Discussion

Many studies have examined the effects of EPO in murine models, particularly with regard to its impact on bone tissue (Kolomansky et al., 2020; Awida et al., 2021; Hiram-Bab et al., 2015; Suresh et al., 2020a; Rauner et al., 2016; Kristjansdottir et al., 2020; Guo et al., 2014; Singbrant et al., 2011b; Shiozawa et al., 2010a; Holstein et al., 2007; Bakhshi et al., 2012; Vasileva et al., 2024). In most of these studies, EPO administration involved multiple intraperitoneal injections or continuous delivery *via* osmotic pumps to simulate chronic or prolonged clinical exposure (Kolomansky et al., 2020; Hiram-Bab et al., 2015; Rauner et al., 2021, 2016). The unique aspect of the current study lies in its focus on the consequences of a single EPO administration, offering insight into the early events that contribute to EPO-induced bone remodeling and bone loss.

Beyond the contrasting skeletal outcomes reported in steady-state *versus* bone regeneration models, as discussed in the Introduction, the direct effect of EPO on osteoblasts remains unresolved. *In vivo*, EPO has been shown to stimulate osteoblastogenesis in bone regeneration contexts but to reduce osteoblast number and function under steady-state conditions (Kolomansky et al., 2020; Shiozawa et al., 2010a). To clarify EPO's direct action on osteoblasts, *in vitro* studies provide valuable information. Several groups have reported that high concentrations of EPO (20–100 U/mL) enhance mineralization and alkaline phosphatase (ALP) activity in both murine and human osteoblast cultures (Li et al., 2015; Rauner et al., 2016; Guo et al., 2014; Balaian et al., 2018; Rölfing et al., 2014; Shiozawa et al., 2010b; Kim et al., 2012). Conversely, lower, more physiological EPO concentrations (0.5–5 mU/mL) were found to inhibit osteoblast differentiation and osteogenic activity (Rauner et al., 2016), aligning with *in vivo* findings of reduced bone formation in steady-state models (Hiram-Bab et al., 2015). In our study as well, osteoblast activity *in vivo* was significantly attenuated on the second day after a single EPO injection (Fig. 5B). These findings support the notion that EPO's effect on osteoblasts is dose-dependent, and that the inhibition observed *in vivo*, even at high doses, may result from differences in pharmacokinetics or indirect mechanisms involving other cell types.

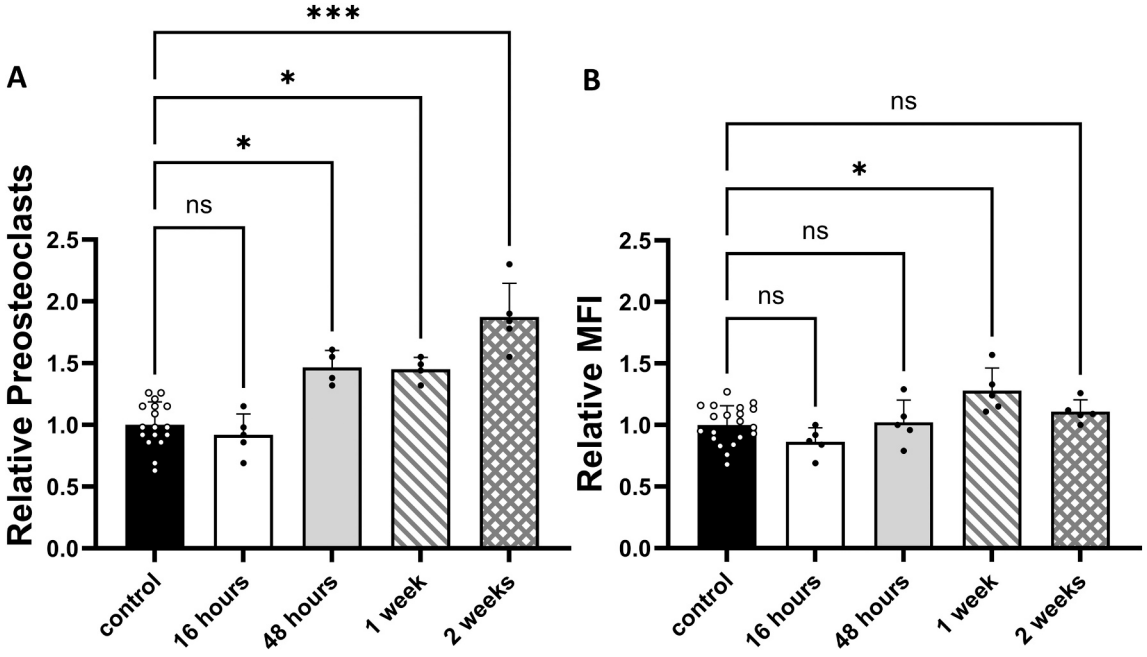

Fig. 4. Flow cytometry analysis of osteoclast progenitors in the BM of EPO-treated mice *vs* control at the designated time points after a single EPO injection. A. Flow cytometry analysis of BM osteoclast progenitors defined as Lin^{-} (CD3^{-}, B220^{-}, Ly6G^{-}, and TER119^{-}) CD11b^{-} Ly6C^{high} CD115^{+}, expressed as percentage of total BM cells. B. The corresponding relative mean fluorescence intensity of CD115 in gated osteoclast progenitors. Data are mean ± SD. ns – nonsignificant *$p < 0.05$.

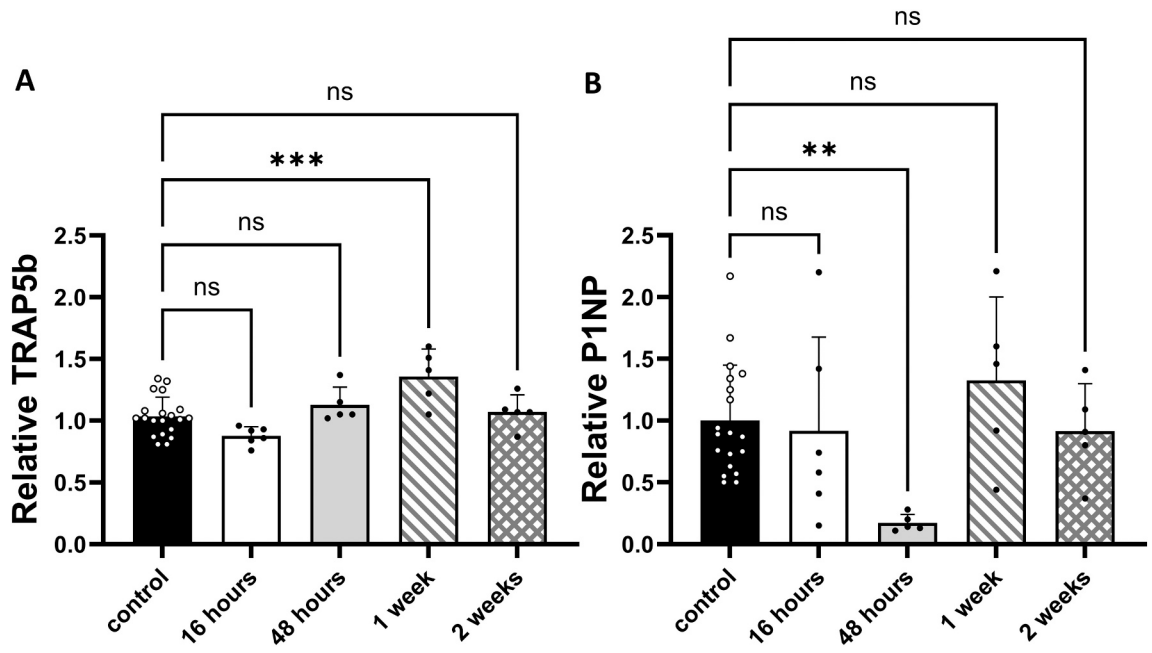

Fig. 5. Serum bone markers of EPO-treated mice *vs* control at the designated time points after a single EPO injection. Data represent protein levels measured by ELISA, shown relative to control. A. Relative serum TRAP5b levels. B. Relative serum P1NP levels. Data are presented as mean ± SD. ns – nonsignificant $^{**}p < 0.01$ $^{***}p < 0.001$.

Our results demonstrate that even a single EPO dose can elicit effects on bone comparable to those induced by repeated injections (Fig. 6). Furthermore, our data point to M-CSF as a central mediator of EPO-induced bone loss. A pronounced M-CSF surge was detected 16 h post-injection, preceding the observed upregulation of osteoclastogenesis and bone resorption, as well as a marked early reduction in bone formation indicated by the sharp drop in P1NP (Fig. 5B). This imbalance between bone resorption and formation likely underlies the rapid loss of trabecular bone observed in EPO-treated mice. Notably, clinical studies have also reported an association between elevated serum EPO levels and decreased bone mass in humans (Kristjansdottir et al., 2020).

Our time-course approach, which included both early (16 and 48 h) and late (1 and 2 weeks) time points, allowed detailed tracking of EPO's temporal effects on bone remodeling. This range was chosen with erythroid maturation in mind, as the process requires several days (Patel and Patel, 2024), prompting us to begin Hgb measurements one week post-injection. A 13 % increase in Hgb, followed by a return to baseline by the second week, confirms that a single EPO dose is sufficient to induce a transient but therapeutically relevant erythropoietic response.

The rapid M-CSF elevation within 16 h post-injection suggests an immediate response of the BM microenvironment to EPO. This M-CSF surge likely facilitates the differentiation and expansion of osteoclast precursors, a process that typically takes approximately 7 days (Awida et al., 2021). Flow cytometry revealed a significant increase (32 %) in $CD115^+$ cells by the second day post-injection. These cells include monocyte-lineage populations that rely on M-CSF for proliferation and survival (Breslin et al., 2013; Cannarile et al., 2017). Although the percentage of $CD115^+$ cells returned to baseline after two weeks, the proportion of osteoclast progenitors remained elevated (Fig. 4A). This sustained expansion may be driven by increased CD115 expression within the precursor population (Fig.4B), enhancing their responsiveness to M-CSF and allowing for their accumulation over the two-week period.

In our study, the osteoclast progenitors were defined as Lin^- $CD11b^-$ $Ly6C^{high}$ $CD115^+$. We focused on the strictly negative fraction to enrich for *bona fide* preosteoclasts and to avoid contamination with $CD11b^{low}$ monocytes that may have limited or no osteoclastogenic potential. This conservative gating strategy is consistent with prior work identifying osteoclast progenitors within the Lin^- $CD11b^{-/low}$ $Ly6C^{high}$ $CD115^+$ compartment (Jacome-Galarza et al., 2013; Jacquin et al., 2006; Das et al., 2020).

Consistent with enhanced osteoclastogenesis, serum TRAP5b levels increased by 19.4 % one week post-injection and subsequently normalized by the second week. This transient elevation aligns with our previous findings of increased osteoclast activity in EPO-treated mice (Hiram-Bab et al., 2015), reinforcing the hypothesis that M-CSF plays a key role in EPO-driven osteoclast expansion.

In parallel, EPO administration also affected the bone-forming compartment of the remodeling cycle. A significant reduction in serum P1NP, a marker of osteoblast activity, was observed two days post-injection. The reduction in P1NP levels two days following EPO administration, rather than after 16 h, suggests an indirect effect of EPO on osteoblasts or may involve differentiation processes that are required before bone formation changes *de facto*. This early decline in P1NP may represent a critical phase of the uncoupling between bone formation and resorption, deviating from the classical tightly coordinated remodeling process (Sims and Martin, 2014). The mechanism behind this suppression and its implications for bone homeostasis warrant further investigation.

A limitation of our study is the inability to perform dynamic histomorphometric analyses, which require dual calcein labeling (7 days and 2 days prior to sacrifice). We acknowledge that dynamic histomorphometry remains the only direct method to discriminate between bone formation and resorption rates, and its absence limits our ability to definitively attribute the observed changes to either process. Given the design of our time-course experiments, this approach was not feasible for most groups. Instead, we relied on serum bone markers (P1NP, TRAP5b), FACS analysis, and protein expression to characterize early remodeling events, which proved effective under the constraints.

The impact of EPO on bone mass became evident one-week post-injection, with a 32.8 % reduction in bone volume to total volume ratio (BV/TV) and a 22.3 % decrease in trabecular number, both of which persisted into the second week (Fig. 6B). These outcomes resemble those observed following repeated EPO injections, suggesting that bone loss is driven by early events rather than cumulative exposure. Interestingly, trabecular thickness was preserved initially and only increased at the

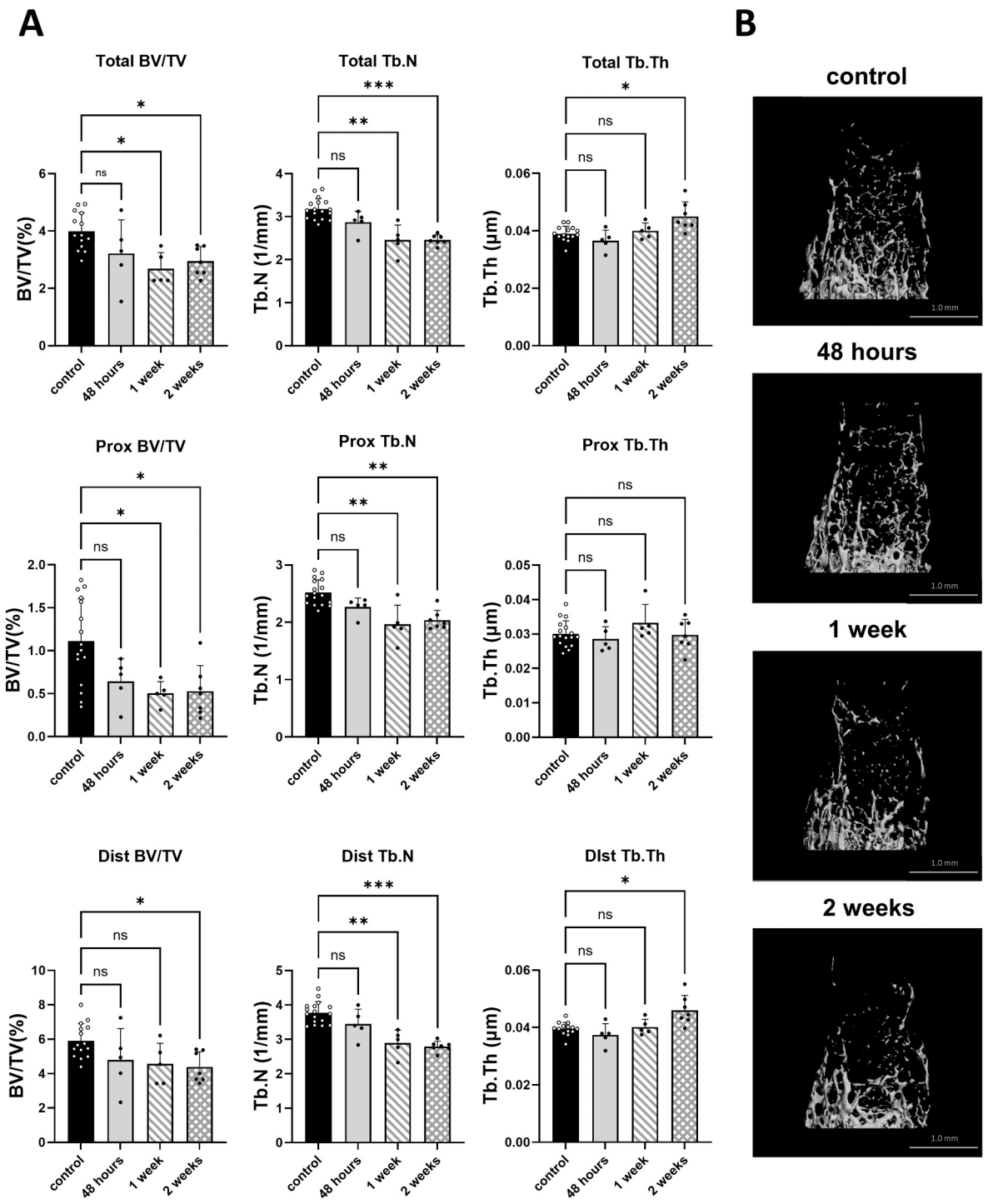

Fig. 6. µCT measurements of EPO-treated mice *vs* control at the designated time points after a single EPO injection. A. µCT measurements (BV/TV, Tb. N, Tb. Th) in the distal femoral trabecular bone of EPO-treated mice *vs* controls at the designated time points after a single EPO injection. Analyses were performed on the entire distal femoral metaphysis (Total), which was further subdivided into proximal (Prox) and distal (Dist) halves. B. Three-dimensional (3D) µCT representative images of the trabecular bone in the distal femur of EPO-treated and control mice. Data are presented as mean ± SD. ns – nonsignificant, $*p < 0.05$, $**p < 0.01$,$***p < 0.001$.

second week (by 15.3 %). This pattern suggests selective loss of thinner trabeculae during the early resorptive phase, with remaining thicker trabeculae serving as scaffolds for subsequent bone formation. As osteoblast activity returns to baseline, new bone may be deposited preferentially along these surviving structures, explaining the concurrent increase in trabecular thickness despite a persistent reduction in number. High-resolution µCT imaging further indicated that structural damage began in the proximal regions of the distal femur, rich in thin trabeculae, while the observed thickening occurred predominantly in the distal half (Fig. 6).

In conclusion, this study provides novel insights into the dynamics of bone remodeling following a single EPO administration. Our findings highlight a rapid and transient imbalance between bone resorption and formation, with M-CSF emerging as a key mediator of EPO-induced bone loss. While the precise cellular mechanisms remain to be determined, the results underscore the importance of considering skeletal effects

Table 2
Additional bone parameters of the distal femoral trabecular bone of EPO-treated mice *vs* controls at the designated time points after a single EPO injection.

Time	48 h					
Treatment	Control			EPO		
Parameter	BMD (%)	Tb.Sp (mm)	Conn.D (1/mm^3)	BMD (%)	Tb.Sp (mm)	Conn.D (1/mm^3)
Total	57.61 ± 7.37	0.32 ± 0.02	35.87 ± 14.29	43.55 ± 12.18	0.35 ± 0.03	29.39 ± 15.71
Proximal	19.16 ± 4.77	0.41 ± 0.02	2.51 ± 2.45	9.88 ± 6.46 *	0.44 ± 0.03	0.33 ± 1.10
Distal	80.25 ± 9.63	0.26 ± 0.02	56.12 ± 22.28	63.84 ± 19.91	0.29 ± 0.04	47.09 ± 25.37
Time	1 week					
Treatment	Control			EPO		
Parameter	BMD (%)	Tb.Sp (mm)	Conn.D (1/mm^3)	BMD (%)	Tb.Sp (mm)	Conn.D (1/mm^3)
Total	68.78 ± 15.39	0.29 ± 0.02	61.51 ± 25.39	24.78 ± 7.37 ***	0.41 ± 0.06 **	0.29 ± 0.02 ***
Proximal	25.63 ± 7.23	0.36 ± 0.03	7.02 ± 4.96	0 ***	0.52 ± 0.08 **	0.90 ± 1.57 *
Distal	94.84 ± 21.51	0.24 ± 0.02	92.33 ± 36.62	47.09 ± 12.34 **	0.35 ± 0.05 **	41.59 ± 18.65 *
Time	2 weeks					
Treatment	Control			EPO		
Parameter	BMD (%)	Tb.Sp (mm)	Conn.D (1/mm^3)	BMD (%)	Tb.Sp (mm)	Conn.D (1/mm^3)
Total	47.68 ± 9.51	0.34 ± 0.01	27.59 ± 8.01	32.08 ± 7.66 **	0.41 ± 0.01 ***	20.59 ± 10.52 *
Proximal	10.78 ± 8.91	0.42 ± 0.03	1.77 ± 4.20	0.93 ± 2.95	0.51 ± 0.03 ***	0.05 ± 0.73
Distal	69.06 ± 8.66	0.28 ± 0.02	42.91 ± 11.84	50.78 ± 10.96 **	0.35 ± 0.01 ***	32.83 ± 17.43

Data are displayed as mean ± SD.
* $p < 0.05$.
** $p < 0.01$.
*** $p < 0.001$.

even after a single EPO exposure. This has important implications for both clinical use and potential misuse of EPO, particularly among high-performance athletes, where even a single dose may significantly compromise bone integrity and elevate fracture risk.

CRediT authorship contribution statement

Anton Gorodov: Writing – original draft, Visualization, Validation, Methodology, Investigation, Formal analysis, Data curation, Conceptualization. **Albert Kolomansky:** Writing – review & editing, Visualization, Validation, Methodology, Data curation, Conceptualization. **Lior Lezerovich:** Data curation. **Michelle Piper:** Data curation. **Nathalie Ben-Califa:** Writing – review & editing, Project administration, Methodology, Data curation. **Yankel Gabet:** Writing – review & editing, Visualization, Validation, Supervision, Resources, Project administration, Methodology, Funding acquisition, Conceptualization. **Drorit Neumann:** Writing – review & editing, Visualization, Validation, Supervision, Resources, Project administration, Funding acquisition, Conceptualization.

Declaration of Generative AI and AI-assisted technologies in the writing process

During the preparation of this work, we used chatGPT to improve language and readability. After using this tool, we reviewed and edited the content as needed. The authors assume full responsibility for the content of the publication.

Declaration of competing interest

The authors declare the following financial interests/personal relationships which may be considered as potential competing interests: Drorit Neumann reports financial support was provided by Israel Science Foundation. Drorit Neumann and Yankel Gabet reports financial support was provided by Sylvan Adams Sports Institute. Drorit Neumann reports financial support was provided by Tel Aviv University The Varda and Boaz Dotan Research Center for Hemato-Oncology Research. If there are other authors, they declare that they have no known competing financial interests or personal relationships that could have appeared to influence the work reported in this paper.

Data availability

The data underlying this article will be shared upon reasonable request to the corresponding author.

Acknowledgements

This research was funded by the Israel Science Foundation (ISF) grant number 1188/21 to DN, The Sylvan Adams Sports Institute, Tel Aviv University (YG and DN) and the Dotan Hemato-oncology Center (DN). DN holds The Lily and Avraham Gildor Chair for the Investigation of Growth Factors.

This work was carried out in partial fulfillment of the requirements for a Ph.D. degree for A.G. from the Gray Faculty of Medical and Health Sciences, Tel Aviv University, Tel Aviv, Israel.

References

Alatalo, S.L., Halleen, J.M., Hentunen, T.A., et al., 2000. Rapid screening method for osteoclast differentiation in vitro that measures tartrate-resistant acid phosphatase 5b activity secreted into the culture medium. Clin. Chem. 46, 1751–1754. https://doi.org/10.1093/clinchem/46.11.1751.

Ali, S.M.E., Hafeez, M.H., Nisar, O., et al., 2022. Role of preoperative erythropoietin in the optimization of preoperative anemia among surgical patients — a systematic review and meta-analysis. Hematol. Transfus. Cell Ther. 44, 76–84. https://doi.org/10.1016/j.htct.2020.12.006.

Amend, S.R., Valkenburg, K.C., Pienta, K.J., 2016. Murine hind limb long bone dissection and bone marrow isolation. JoVE, 53936. https://doi.org/10.3791/53936.

Awida, Z., Bachar, A., Saed, H., et al., 2021. The non-erythropoietic EPO analogue cibinetide inhibits osteoclastogenesis in vitro and increases bone mineral density in mice. Int. J. Mol. Sci. 23, 55. https://doi.org/10.3390/ijms23010055.

Bakhshi, H., Kazemian, G., Emami, M., et al., 2012. Local erythropoietin injection in tibiofibular fracture healing. Trauma Mon. 17, 386–388. https://doi.org/10.5812/traumamon.7099.

Balaian, E., Wobus, M., Weidner, H., et al., 2018. Erythropoietin inhibits osteoblast function in myelodysplastic syndromes via the canonical Wnt pathway. Haematologica 103, 61–68. https://doi.org/10.3324/haematol.2017.172726.

Biboulet, P., Motais, C., Pencole, M., et al., 2020. Preoperative erythropoietin within a patient blood management program decreases both blood transfusion and postoperative anemia: a prospective observational study. Transfusion 60, 1732–1740. https://doi.org/10.1111/trf.15900.
Bouxsein, M.L., Boyd, S.K., Christiansen, B.A., et al., 2010. Guidelines for assessment of bone microstructure in rodents using micro–computed tomography. J. Bone Miner. Res. 25, 1468–1486. https://doi.org/10.1002/jbmr.141.
Breslin, W.L., Strohacker, K., Carpenter, K.C., et al., 2013. Mouse blood monocytes: standardizing their identification and analysis using CD115. J. Immunol. Methods 390, 1–8. https://doi.org/10.1016/j.jim.2011.03.005.
Cai, T., Chen, S., Wu, C., et al., 2023. Erythropoietin suppresses osteoblast apoptosis and ameliorates steroid-induced necrosis of the femoral head in rats by inhibition of STAT1-caspase 3 signaling pathway. BMC Musculoskelet. Disord. 24, 894. https://doi.org/10.1186/s12891-023-07028-y.
Cannarile, M.A., Weisser, M., Jacob, W., et al., 2017. Colony-stimulating factor 1 receptor (CSF1R) inhibitors in cancer therapy. J. Immunother. Cancer 5, 53. https://doi.org/10.1186/s40425-017-0257-y.
Cho, B.C., Serini, J., Zorrilla-Vaca, A., et al., 2019. Impact of preoperative erythropoietin on allogeneic blood transfusions in surgical patients: results from a systematic review and meta-analysis. Anesth. Analg. 128, 981–992. https://doi.org/10.1213/ANE.0000000000004005.
Das, A., Wang, X., Kang, J., et al., 2020. Monocyte subsets with high osteoclastogenic potential and their epigenetic regulation orchestrated by IRF8. J. Bone Miner. Res. 36, 199–214. https://doi.org/10.1002/jbmr.4165.
Eckardt, K.U., Koury, S.T., Tan, C.C., et al., 1993. Distribution of erythropoietin producing cells in rat kidneys during hypoxic hypoxia. Kidney Int. 43, 815–823. https://doi.org/10.1038/ki.1993.115.
Fleetwood, A.J., Achuthan, A., Hamilton, J.A., 2016. Colony stimulating factors (CSFs). In: Encyclopedia of Immunobiology. Elsevier, pp. 586–596. https://doi.org/10.1016/B978-0-12-374279-7.10015-3.
Forbes, C.A., Worthy, G., Harker, J., et al., 2014. Dose efficiency of erythropoiesis-stimulating agents for the treatment of patients with chemotherapy-induced anemia: a systematic review. Clin. Ther. 36, 594–610.e4. https://doi.org/10.1016/j.clinthera.2014.02.007.
Gassmann, M., Heinicke, K., Soliz, J., Ogunshola, O.O., 2003. Non-erythroid functions of erythropoietin. Adv. Exp. Med. Biol. 543, 323–330. https://doi.org/10.1007/978-1-4419-8997-0_22.
Guo, L., Luo, T., Fang, Y., et al., 2014. Effects of erythropoietin on osteoblast proliferation and function. Clin. Exp. Med. 14, 69–76. https://doi.org/10.1007/s10238-012-0220-7.
Hadjidakis, D.J., Androulakis, I.I., 2006. Bone remodeling. Ann. N. Y. Acad. Sci. 1092, 385–396. https://doi.org/10.1196/annals.1365.035.
Hiram-Bab, S., Liron, T., Deshet-Unger, N., et al., 2015. Erythropoietin directly stimulates osteoclast precursors and induces bone loss. FASEB J. 29, 1890–1900. https://doi.org/10.1096/fj.14-259085.
Holstein, J.H., Menger, M.D., Scheuer, C., et al., 2007. Erythropoietin (EPO) — EPO-receptor signaling improves early endochondral ossification and mechanical strength in fracture healing. Life Sci. 80, 893–900. https://doi.org/10.1016/j.lfs.2006.11.023.
Hume, D.A., MacDonald, K.P.A., 2012. Therapeutic applications of macrophage colony-stimulating factor-1 (CSF-1) and antagonists of CSF-1 receptor (CSF-1R) signaling. Blood 119, 1810–1820. https://doi.org/10.1182/blood-2011-09-379214.
Jacome-Galarza, C.E., Lee, S.-K., Lorenzo, J.A., Aguila, H.L., 2013. Identification, characterization, and isolation of a common progenitor for osteoclasts, macrophages, and dendritic cells from murine bone marrow and periphery. J. Bone Miner. Res. 28, 1203–1213. https://doi.org/10.1002/jbmr.1822.
Jacquin, C., Gran, D.E., Lee, S.K., et al., 2006. Identification of multiple osteoclast precursor populations in murine bone marrow. J. Bone Miner. Res. 21, 67–77. https://doi.org/10.1359/JBMR.051007.
Jung, Y., Ziegler, A., Shiozawa, Y., et al., 2008. Erythropoietin stimulates bone formation in vivo by targeting both HSCs and MSCs. Blood 112, 321. https://doi.org/10.1182/blood.V112.11.321.321.
Kim, J., Jung, Y., Sun, H., et al., 2012. Erythropoietin mediated bone formation is regulated by mTOR signaling. J. Cell. Biochem. 113, 220–228. https://doi.org/10.1002/jcb.23347.
Kolomansky, A., Hiram-Bab, S., Ben-Califa, N., et al., 2020. Erythropoietin mediated bone loss in mice is dose-dependent and mostly irreversible. Int. J. Mol. Sci. 21, 3817. https://doi.org/10.3390/ijms21113817.
Kristjansdottir, H.L., Lewerin, C., Lerner, U.H., et al., 2020. High plasma erythropoietin predicts incident fractures in elderly men with normal renal function: the MrOS Sweden cohort. J. Bone Miner. Res. 35, 298–305. https://doi.org/10.1002/jbmr.3900.
Li, C., Shi, C., Kim, J., et al., 2015. Erythropoietin promotes bone formation through EphrinB2/EphB4 signaling. J. Dent. Res. 94, 455–463. https://doi.org/10.1177/0022034514566431.
Lipšic, E., Schoemaker, R.G., Van Der Meer, P., et al., 2006. Protective effects of erythropoietin in cardiac ischemia. J. Am. Coll. Cardiol. 48, 2161–2167. https://doi.org/10.1016/j.jacc.2006.08.031.
Liu, X., Zhou, M., Wu, Y., et al., 2024. Erythropoietin regulates osteoclast formation via up-regulating PPARγ expression. Mol. Med. 30, 151. https://doi.org/10.1186/s10020-024-00931-7.
Lundby, C., Thomsen, J.J., Boushel, R., et al., 2007. Erythropoietin treatment elevates haemoglobin concentration by increasing red cell volume and depressing plasma volume. J. Physiol. 578, 309–314. https://doi.org/10.1113/jphysiol.2006.122689.
Melkko, J., Kauppila, S., Niemi, S., et al., 1996. Immunoassay for intact amino-terminal propeptide of human type I procollagen. Clin. Chem. 42, 947–954. https://doi.org/10.1093/clinchem/42.6.947.
Munting, K.E., Klein, A.A., 2019. Optimisation of pre-operative anaemia in patients before elective major surgery – why, who, when and how? Anaesthesia 74, 49–57. https://doi.org/10.1111/anae.14466.
Panjeta, M., Tahirovic, I., Karamehic, J., et al., 2015. The relation of erythropoietin towards hemoglobin and hematocrit in varying degrees of renal insufficiency. Mater. Sociomed. 27, 144–148. https://doi.org/10.5455/msm.2015.27.144-148.
Patel, S., Patel, J.B., 2024. Epoetin alfa. In: StatPearls. StatPearls Publishing, Treasure Island (FL).
Peng, B., Kong, G., Yang, C., Ming, Y., 2020. Erythropoietin and its derivatives: from tissue protection to immune regulation. Cell Death Dis. 11, 1–12. https://doi.org/10.1038/s41419-020-2276-8.
Rauner, M., Franke, K., Murray, M., et al., 2016. Increased EPO levels are associated with bone loss in mice lacking PHD2 in EPO-producing cells. J. Bone Miner. Res. 31, 1877–1887. https://doi.org/10.1002/jbmr.2857.
Rauner, M., Murray, M., Thiele, S., et al., 2021. Epo/EpoR signaling in osteoprogenitor cells is essential for bone homeostasis and Epo-induced bone loss. Bone Res. 9, 42. https://doi.org/10.1038/s41413-021-00157-x.
Robinson, N., Giraud, S., Saudan, C., et al., 2006. Erythropoietin and blood doping. Br. J. Sports Med. 40 (Suppl. 1), i30–i34. https://doi.org/10.1136/bjsm.2006.027532.
Rölfing, J.H.D., Jensen, J., Jensen, J.N., et al., 2014. A single topical dose of erythropoietin applied on a collagen carrier enhances calvarial bone healing in pigs. Acta Orthop. 85, 201–209. https://doi.org/10.3109/17453674.2014.889981.
Rosencher, N., Poisson, D., Albi, A., et al., 2005. Two injections of erythropoietin correct moderate anemia in most patients awaiting orthopedic surgery. Can. J. Anesth./J. Can. Anesth. 52, 160–165. https://doi.org/10.1007/bf03027722.
Shiozawa, Y., Jung, Y., Ziegler, A.M., et al., 2010a. Erythropoietin couples hematopoiesis with bone formation. PLoS One 5, e10853. https://doi.org/10.1371/journal.pone.0010853.
Shiozawa, Y., Jung, Y., Ziegler, A.M., et al., 2010b. Erythropoietin couples hematopoiesis with bone formation. PLoS One 5, e10853. https://doi.org/10.1371/journal.pone.0010853.
Sims, N.A., Martin, T.J., 2014. Coupling the activities of bone formation and resorption: a multitude of signals within the basic multicellular unit. BoneKEy Rep. 3. https://doi.org/10.1038/bonekey.2013.215.
Singbrant, S., Russell, M.R., Jovic, T., et al., 2011a. Erythropoietin couples erythropoiesis, B-lymphopoiesis, and bone homeostasis within the bone marrow microenvironment. Blood 117, 5631–5642. https://doi.org/10.1182/blood-2010-11-320564.
Singbrant, S., Russell, M.R., Jovic, T., et al., 2011b. Erythropoietin couples erythropoiesis, B-lymphopoiesis, and bone homeostasis within the bone marrow microenvironment. Blood 117, 5631–5642. https://doi.org/10.1182/blood-2010-11-320564.
Singhal, N.K., Alkhayer, K., Shelestak, J., et al., 2018. Erythropoietin upregulates brain hemoglobin expression and supports neuronal mitochondrial activity. Mol. Neurobiol. 55, 8051–8058. https://doi.org/10.1007/s12035-018-0971-6.
Šromová, V., Sobola, D., Kaspar, P., 2023. A brief review of bone cell function and importance. Cells 12, 2576. https://doi.org/10.3390/cells12212576.
Suresh, S., Lee, J., Noguchi, C.T., 2020a. Erythropoietin signaling in osteoblasts is required for normal bone formation and for bone loss during erythropoietin-stimulated erythropoiesis. FASEB J. 34, 11685–11697. https://doi.org/10.1096/fj.202000888R.
Suresh, S., Wright, E.C., Wright, D.G., et al., 2020b. Erythropoietin treatment and the risk of hip fractures in hemodialysis patients. J. Bone Miner. Res. 36, 1211–1219. https://doi.org/10.1002/jbmr.4297.
Tsang, K., Liu, H., Yang, Y., et al., 2019. Defective circadian control in mesenchymal cells reduces adult bone mass in mice by promoting osteoclast function. Bone 121, 172–180. https://doi.org/10.1016/j.bone.2019.01.016.
van der Meer, P., Lipsic, E., 2006. Erythropoietin: repair of the failing heart. J. Am. Coll. Cardiol. 48, 185–186. https://doi.org/10.1016/j.jacc.2006.04.007.
Vasileva, R., Chaprazov, T., Milanova, A., 2024. Effects of erythropoietin-promoted fracture healing on bone turnover markers in cats. JFB 15, 106. https://doi.org/10.3390/jfb15040106.
Weltert, L., D'Alessandro, S., Nardella, S., et al., 2010. Preoperative very short-term, high-dose erythropoietin administration diminishes blood transfusion rate in off-pump coronary artery bypass: a randomized blind controlled study. J. Thorac. Cardiovasc. Surg. 139, 621–627. https://doi.org/10.1016/j.jtcvs.2009.10.012.
Westenbrink, B.D., Lipšic, E., Van Der Meer, P., et al., 2007. Erythropoietin improves cardiac function through endothelial progenitor cell and vascular endothelial growth factor mediated neovascularization. Eur. Heart J. 28, 2018–2027. https://doi.org/10.1093/eurheartj/ehm177.
Wu, H., Liu, X., Jaenisch, R., Lodish, H.F., 1995. Generation of committed erythroid BFU-E and CFU-E progenitors does not require erythropoietin or the erythropoietin receptor. Cell 83, 59–67. https://doi.org/10.1016/0092-8674(95)90234-1.
Yoo, Y.-C., Shim, J.-K., Kim, J.-C., et al., 2012. Effect of single recombinant human erythropoietin injection on transfusion requirements in preoperatively anemic patients undergoing valvular heart surgery. Surv. Anesthesiol. 56, 106–107. https://doi.org/10.1097/01.sa.0000413395.98867.60.